

Article

Optimization of Cab Vibration Comfort for Construction Machinery Based on Multi-Target Regression Forests

Chao Zhuang ¹, Hansheng Wen ², Xiangyu Ni ¹, Da Zhang ¹, Yangyang Bao ² and Haibo Huang ^{2,*}

¹ State Key Laboratory of Intelligent Manufacturing of Advanced Construction Machinery, Xuzhou Construction Machinery Group, Xuzhou 211162, China

² School of Mechanical Engineering, Southwest Jiaotong University, Chengdu 610031, China

* Correspondence: huanghaibo214@my.swjtu.edu.cn

Abstract: With the increasing awareness of the importance of environmental protection and the fierce competition in the construction machinery market, improving the vibration comfort of a whole construction machine has become a new focus of competition; therefore, optimizing the performance of cab mounts has become an urgent problem to be solved. At present, the problems of low modeling efficiency, serious technical difficulties, and long development cycles exist in the design and optimization of cab mounts. In this paper, a multi-target regression forests method is introduced into the design and optimization of the construction machinery installation system, which circumvents the traditional complex modeling process and establishes a mapping relationship between cab assembly parameters and the mounts' stiffness, as well as introduces the system decoupling rate and vibration isolation rate as the boundary conditions. Furthermore, the MRFs method is compared and evaluated with MLRP and Multi-SVR prediction results. Finally, a complete, accurate, and efficient design method for the cab mount system optimization is developed, improving the decoupling rate and vibration isolation rate of the cab system. This design method can predict the stiffness of the mounts in multiple directions.

Keywords: MRFs; vibration comfort; optimization; construction machinery



Citation: Zhuang, C.; Wen, H.; Ni, X.; Zhang, D.; Bao, Y.; Huang, H. Optimization of Cab Vibration Comfort for Construction Machinery Based on Multi-Target Regression Forests. *Machines* **2022**, *10*, 1148. <https://doi.org/10.3390/machines10121148>

Academic Editor: Davide Astolfi

Received: 28 October 2022

Accepted: 25 November 2022

Published: 1 December 2022

Publisher's Note: MDPI stays neutral with regard to jurisdictional claims in published maps and institutional affiliations.



Copyright: © 2022 by the authors. Licensee MDPI, Basel, Switzerland. This article is an open access article distributed under the terms and conditions of the Creative Commons Attribution (CC BY) license (<https://creativecommons.org/licenses/by/4.0/>).

1. Introduction

With the continuous improvement of environmental awareness and related laws and regulations, whether in the automotive industry or the construction machinery industry, more and more customers are increasingly concerned about vibration and noise hazards [1], which has led to the development of product design for sound and vibration comfort (noise, vibration, and harshness, NVH), issues of great importance [2]. At present, the construction machinery market is increasingly competitive, and the performance cost of the same class of models in the conventional aspects is getting closer and closer. Therefore, the new competition and technology directions are focused on improving the level of vibration comfort of the whole vehicle.

As the main interaction mechanism of the driver, the vibration performance of the cab is directly felt. In the process of operation, a cab vibration level that is too high will lead to a variety of adverse reactions from the driver, such as lack of energy, slow response, etc. [3,4]. Therefore, cab design should consider not only safety and economy but also comfort. Cab mounts as the central system of cab vibration isolation, as well as their impact on the whole vehicle's vibration comfort performance, is of great importance. In order to improve the driver's ride comfort, in addition to considering the main vibration sources such as work devices, engines, tracks, etc., vibration must be reduced from the source, and isolating the vibration source of the cab's vibration has also become a vibration comfort improvement that can no longer be ignored. By optimizing the design of the cab mounts, the vibrations transmitted from the frame to the cab can be further reduced [5]. Therefore,

the performance of the cab mounts directly affects the level of cab vibration response and plays a vital role in improving cab vibration comfort [6].

The process of cab parameters information acquisition as well as the matching analysis and optimization of mount systems requires in-depth theoretical research combined with experimental design and finite element analyses. In this process, the traditional mount system design and optimization processes also face the following obstacles: on one hand, the technical difficulties, meaning that in an actual project of construction machinery cab mount system design and optimization, there are many conflicting requirements and constraints that need to be met simultaneously; on the other hand, cab mount system parameters are numerous, and small parameter changes will lead to a significant change in the performance of the mount system. This brings incredible technical difficulties to the improvement of the vibration isolation performance of the mounts. In addition, in the optimization of the cab mount system, it is necessary to carry out decoupling optimization, vibration isolation optimization, and robustness optimization based on the vehicle's coordinate system [7], which requires repeated iterations or repeated tuning with the help of cab simulation models and mathematical models, which cannot achieve the purpose of rapid optimization, in particular due to the challenge of meeting the accuracy requirements of multiple mounts and an optimal matching of stiffness in different directions, resulting in a long development period for the mount system and low efficiency.

In this paper, data mining technology is introduced based on the design and optimization of the mount system. Indicators such as system decoupling and vibration isolation rates are introduced as boundary conditions for evaluation. In the following, the current status of the research will be described from two aspects: the design method and the evaluation method of the mount stiffness of construction machinery cabs.

Today, the methods for predicting the stiffness of construction machinery cab mounts include traditional finite element calculation methods based on mechanism and data mining methods, in turn based on data drive [8,9]. As a nonlinear material, unlike metals, rubber mounts do not have a suitable formula for calculating stiffness [10]; with the maturity of the hyper-elasticity theory of rubber materials and the development of computer technology, finite element software such as ADINA and ABAQUS can be applied to calculate and study rubber mounts. In the 1940s, Strachousky and RicherHarding composed a damping mechanism composed of rubber and a hydraulic damping device and applied for a patent [11]. Muller of Germany obtained various structural parameters of rubber mounts by the finite element analysis method, established an axisymmetric finite element model of the main rubber spring, and calculated the curve of force and deformation of the main rubber spring [12]. Foumani used ANSYS to calculate an axisymmetric rubber mainspring volume flexibility problem. The method for setting the boundary conditions and the final results of the simulation are given in the paper [13]. Judhaji, in order to analyze the effect of different vibration modes on ride comfort, built a whole vehicle model for simulation and improved the ride comfort significantly by changing the mounts' position relative to the body [14]. AlaoJ.Vieira Neto analyzed the effects of cab mount system stiffness and damping on front longitudinal and transverse accelerations, vertical seat displacement, vertical seat velocity, and vertical seat acceleration using a large number of experiments, and then designed the parameters of the cab mount system according to the analysis results, which reduced the displacement and acceleration of the cab to a great extent [15]. Based on the relevant studies of the above scholars, the use of the finite element method requires an extensive theoretical study of the suspension rubber's stiffness and cab system combined with experimental design for analysis, as this method leads to a time-consuming and inefficient modeling process and is not conducive to rapid optimization [16]. In contrast to the traditional finite element method, the data mining method for predicting the mounts' stiffness can discard the complicated investigation and complex modeling process and significantly improve the prediction and optimization efficiency. In order to identify the positive and negative mechanical models of magnetorheological hydraulic mounts, Deng Zhaoxue of Chongqing University uses the dynamic characteristics of magnetorheological

mounts as training data and compares the model identification accuracy of two algorithms, namely the BP neural network and the GA–BP neural network. The results show that magnetorheological hydraulic mounts' positive and negative models using the GA–BP neural network have a faster convergence speed and higher identification accuracy. This method helps control the magnetorheological mounts. Rheological mounts are applied to the control of the system [17]. Using loudness, roughness, sharpness, jitter, and speech intelligibility as input parameters and subjective evaluation scores as output parameters, Fang Yuan, of Tongji University, established a prediction model for powertrain noise quality of electric vehicles using a support vector machine algorithm. This optimized the model using a particle swarm algorithm, and the results showed that the prediction model has high accuracy with an average error of only 2% [18]. Cao used the advanced hybrid neural network (AHNN) friction component model to train the model with the data obtained from the powertrain dynamometer test bench and finally predicted the dynamics parameters of the gearbox when shifting [19]. Paweł Cichosz used an improved decision tree model to emulate the driver's behavior in a racing car simulation, balancing accuracy when the machine works with logic to when a human is working [20]. MarielaCerrada used a genetic algorithm and a random forest classifier for gearbox fault detection with a classification accuracy of more than 97% [21]. Yiqi Lu proposed an EV charging load prediction method based on the random forest algorithm and individual charging station load data for the increasing charging demand of EVs, determined the form of current data to be applied in the algorithm, and verified the accuracy and reliability of the prediction algorithm [22]. This shows that it is feasible to use data mining methods to predict mount stiffness.

At the same time, the stiffness of the predicted mount needs to be evaluated. The evaluation methods of the cab mounts can be divided into the following two categories: one of them is the mount system level, and the stiffness of the mounts is constrained by the decoupling rate as the boundary condition [23]. The decoupling rate of the main vibration directions is maximized by setting the stiffness of the appropriate mount. The second is the whole vehicle level, which mainly depends on the vibration isolation performance analysis of the system [24], where the vibration transmission goes through the frame and into the cab system, and again the stiffness of the mounts is constrained by the vibration isolation performance as a boundary condition. The above study proves the feasibility of data mining technology for mount stiffness prediction. For a nonlinear, continuous numerical variable such as mount system stiffness, the mapping relationship between powertrain parameters and mount stiffness can be established by using data mining methods, and engineering evaluation indices such as decoupling rate and cab mount system vibration isolation rate are introduced as the boundary conditions of the multiple regression prediction models. The traditional complex modeling process is circumvented, and the direct prediction of mount stiffness is achieved for the rapid optimization of the mount system.

After the research mentioned above, relevant scholars conducted certain research on cab mount stiffness prediction and achieved effective results. However, the following common problems still exist in the prediction and evaluation of the cab mount stiffness of construction machinery.

(1) Most previous studies on cab mount stiffness prediction used traditional finite element methods, leading to increased modeling complexity and reduced prediction and optimization efficiency. Some scholars use data mining methods based on the data drive, in which multi-output models are not introduced. The single-output prediction results lead to low confidence in the predicted stiffness of the mounts due to the correlation between the isotropic stiffness of each mount.

(2) Previous studies on the use of MRFs for cab mount stiffness prediction have rarely been reported. The related mount optimization study did not include vibration isolation rate and decoupling rate indices for further evaluation and analysis of the engineering significance and reasonableness of the model. Using it as the boundary condition of the regression model can improve the feasibility of the stiffness of the predicted mount under engineering practice.

Based on the above analysis, this paper takes the construction machinery cab mount systems as the research object, circumvents the traditional complicated modeling process, proposes to introduce multi-target regression forests (MRFs) in the design and optimization design of the mount system, and integrates the mount parameters with the MRFs method to achieve multi-point mount stiffness prediction. In addition, engineering evaluation indices such as system decoupling rate and vibration isolation rate are used as boundary conditions. At the same time, two other multi-output regression methods (multi-layer perception regression, multiple-output support vector machine regression) are compared to find a relatively satisfactory multi-objective prediction model method. A set of high-confidence mounting system stiffness prediction models is established to avoid the complex modeling process. The mapping relationship between cab parameters and mounting stiffness is established, which solves the problems of technical difficulty, low data mining rate, and long development period in the development of the mount systems, and is applied to the optimization of the cab mount systems in engineering.

2. Multi-Target Regression Forests Model

2.1. Introduction of MRFs Model

From the current state of research on the design of the mounts of the cab of construction machinery, it can be seen that the optimized design of the mounts is mainly focused on the optimization of the stiffness of the mounts. In dynamics modeling, the mounts are usually simplified to three mutually perpendicular linear springs, and the mounts individually provide stiffness in each direction. Due to the correlation of the isotropic stiffness between the mounts [25], when the mount stiffness is used as a prediction target for model tuning, it will inevitably affect other models, so it is necessary to consider the correlation between the targets and establish a multi-output model of mount stiffness. The advantages of multi-objective regression mainly lie in that a multi-objective regression model is usually smaller than a model with multiple single objectives. The multi-objective model can better identify the dependencies between different target variables, and the model prediction is better.

MRFs are trees that can predict multiple consecutive objectives at the same time. Internally, it is a binary tree structure that divides the data into two subsets with an optimization basis at each node, and the optimization basis for multiple objectives is to replace the sum of the squared errors of a single variable with the sum of the squared errors of multiple variables, repeating the division process until the stopping condition is satisfied, and finally generating a decision tree with the median or mean value of the leaf nodes as the prediction result [26]. The MRFs algorithm can better handle the interaction between the input features of the mount stiffness prediction model, and the generated results are highly interpretable. Moreover, the algorithm's robustness is good when adding noisy data or feature changes during the MRFs model-building process, which can automatically detect the interactions between variables and handle the missing values in the element variables with minimal information loss [27].

Let us suppose the data set D contains N data samples, the data set D is $D = \{(x^{(1)}, y^{(1)}), \dots, (x^{(N)}, y^{(N)})\}$. The feature set has r dimensions, denoted as $x^l = (x_1^l, \dots, x_j^l, \dots, x_r^l)$. For the input variables and the corresponding output variables, the training set is divided into two subsets when the j th feature vector and the corresponding fetch s are chosen as the division variable and the division point, which is defined as:

$$R_1(j, s) = \{x \mid x^{(j)} \leq s\} \quad (1)$$

$$R_2(j, s) = \{x \mid x^{(j)} > s\} \quad (2)$$

In the above equation: $R_1(j,s)$ is the set of features taking values less than or equal to s ; $R_2(j,s)$ is the set of features taking values greater than s ; the optimal division variables and the optimal division points are required, i.e., to find:

$$\min_{j,s} \left[\min_{R_1} \sum_{x_i \in R_1(j,s)} \sum_{i=1}^d (y_i - \bar{y}_1)^2 + \min_{R_2} \sum_{x_i \in R_2(j,s)} \sum_{i=1}^d (y_i - \bar{y}_2)^2 \right] \quad (3)$$

$$\bar{y}_1 = \text{ave}(y_i | x_i \in R_1(j,s)) \quad (4)$$

$$\bar{y}_2 = \text{ave}(y_i | x_i \in R_2(j,s)) \quad (5)$$

In the above equation: y_i is the actual value corresponding to the input variable x_i ; which must traverse the variable j and find the value of j and s , which makes the minimum value, that is, the optimal division variable and the optimal division point, divide the region with the selected optimal division variable and the optimal division point, and derive the output value.

$$\hat{c}_m = \frac{1}{N_m} \sum_{x \in R_m(j,s)} y_i, m = 1, 2 \quad (6)$$

The process is repeated, dividing the input set into two subsets each time until the stopping condition is satisfied. Finally, the input set is divided into M regions, namely R_1, R_2, \dots, R_M , generating a decision tree.

$$f(x) = \sum_{m=1}^M \hat{c}_m I(x \in R_m) \quad (7)$$

A random forest dealing with regression problems can also be referred to as a regression forest. A regression forest consists of T regression trees, whose predicted values can be calculated by Equation (8).

$$p_t = \frac{1}{T} \sum_{i=1}^T f(x)_i \quad (8)$$

In the above equation: p_t is the predicted value of the test sample; $f(x)_i$ is the predicted value of the i th tree.

2.2. Method for Predicting Cab Mount Stiffness Based on MRFs

Taking the cab mount system of construction machinery as the object of study, the left front mounts, right front mounts, left rear mounts, and right rear mounts are arranged. The arrangement of the corresponding mount system is flat-mounted, and the stiffness coordinate system of each elastic support is parallel to the cab's center-of-mass coordinate system. The locations of the cab and suspension are shown in Figure 1. The factors affecting the performance of the cab mount system include the inertia parameters of the cab's center-of-mass coordinates, the installation coordinates of each mount, the installation angle, and the stiffness of each elastic spindle [28,29].

In the multi-output regression model of the mounts, the cab mass m , the rotational inertia I_{ij} ($i, j = x, y, z$), and the difference in the coordinates of the mounts C_{mm} ($m = a, b, c, d$; $n = x, y, z$) are used as input parameters, where x, y , and z represent the three directions, and a, b, c , and d represent the different mounts. As shown in Table 1, the above 19-dimensional parameters are used as the input of the multi-output regression model, and the output parameters are the stiffnesses of the four mounts in three directions, with a total of 12 target parameters. The model has a total of 50 sets of data, 80% of which are used as the training set and 20% of which are used as the test set. Since the selected object is a flat-mounted mount system, the mounting angle is not used as a feature parameter. The flow of MRFs-based cab mount stiffness prediction is shown in Figure 2.

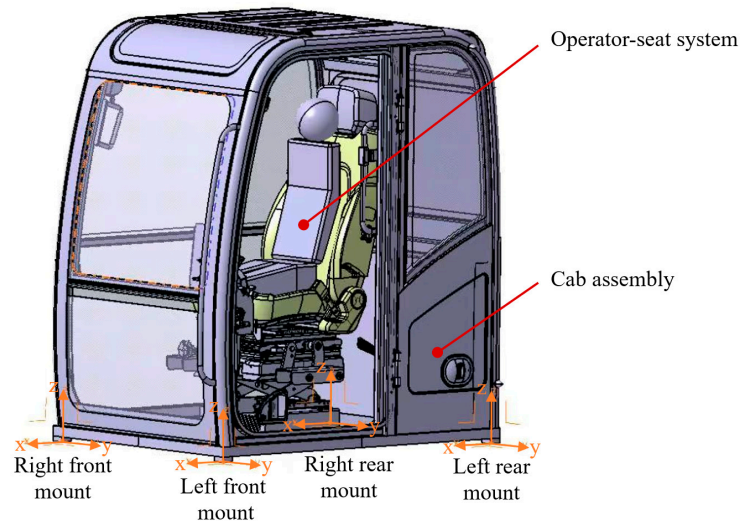


Figure 1. Construction machinery cab.

Table 1. Cab mounts model input feature parameters.

Characteristic Parameters	I_{xx} (kg·m ²)	I_{yy} (kg·m ²)	I_{zz} (kg·m ²)	I_{xy} (kg·m ²)	I_{yz} (kg·m ²)	I_{xz} (kg·m ²)	m (kg)
	538	733	425	0.49	−5.6	15.7	759.23
	C_{ax} (mm)	C_{ay} (mm)	C_{az} (mm)	C_{bx} (mm)	C_{by} (mm)	C_{bz} (mm)	
	856.727	−365	−422.651	857.727	334.271	−422.651	
	C_{cx} (mm)	C_{cy} (mm)	C_{cz} (mm)	C_{dx} (mm)	C_{dy} (mm)	C_{dz} (mm)	
	−623.273	−365.229	−422.651	−623.273	334.271	−422.651	

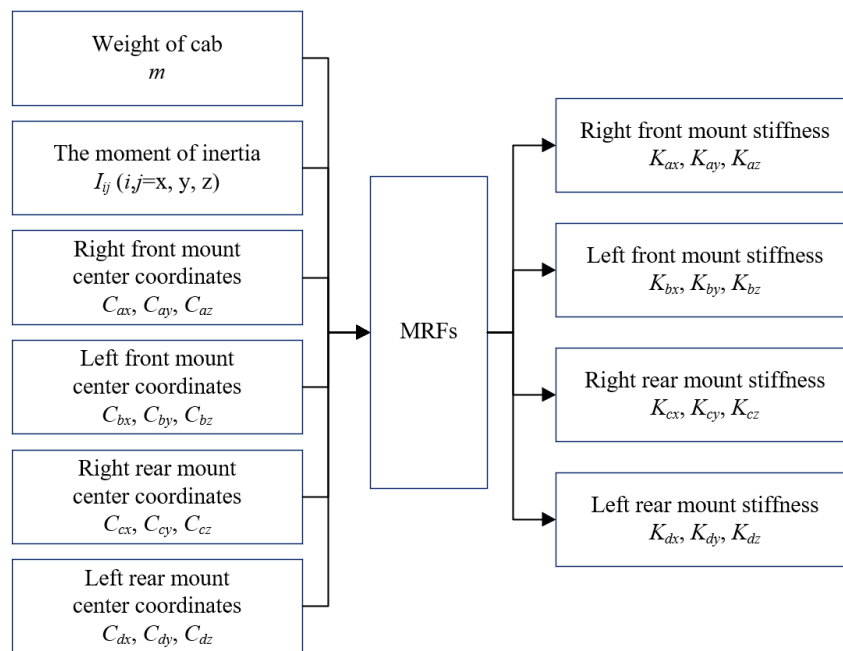


Figure 2. MRFs-based cab mount stiffness prediction process.

3. Prediction and Validation of Cab Mount Stiffness Based on MRFs

As shown in Figure 3, the process of the construction machinery cab mount design evaluation method is shown. In order to establish a high-quality excavation model, the quality of the data must meet the requirements of accuracy, interpretability, and credibility, and the data must be pre-processed. First, for the samples with missing mount-position coordinates, the mount-position coordinates are deduced according to the torque axis theory. The data sets with high correlation coefficients are integrated and downsampled according to the Pearson correlation coefficient calculation method. Finally, the data are downsampled by applying the principal component analysis method to achieve the purpose of simplifying the model and preventing the occurrence of overfitting. At the same time, the MRFs data mining algorithm is introduced in the design of the stiffness of the mount, and the mount parameters are integrated with the MRFs method. The system decoupling rate, as well as the vibration isolation rate and other indices, are used as boundary conditions. The stiffness of the four mounts of the cab in 12 directions is finally output as the target.

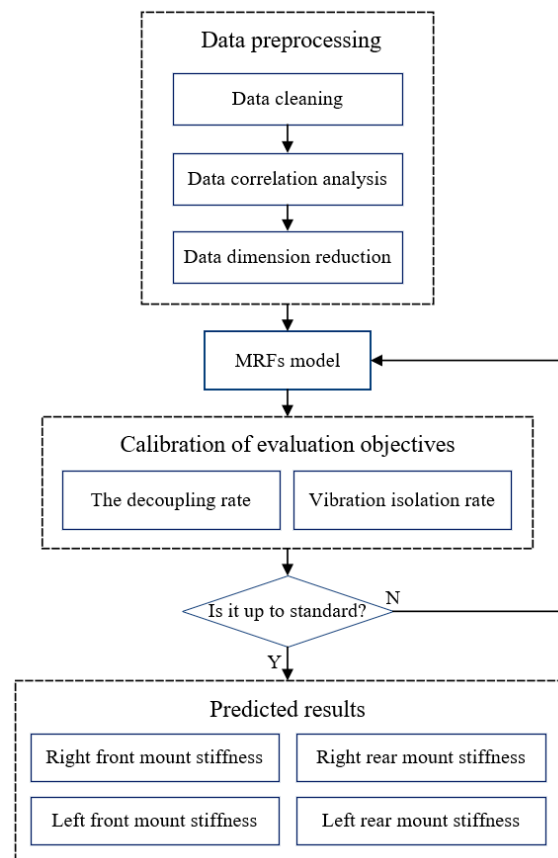


Figure 3. MTRs model optimization process.

3.1. Data Preprocessing

1. Data Cleaning

Collecting parameters of the cab mount system includes measuring inertia parameters by the three-line pendulum method, the moment balance method, and the compound pendulum method [30]. The static stiffness of the mount is measured by the Dynamic Testing Machine Model UD-3600-1, which may lead to missing or incomplete data during the simulation or field measurement of the coordinates of the mounts, so the data cleaning process must verify the missing data and correct the filling. The data set of the mount system has specific correlation compared with other traditional structure data sets, and the engineering theory can fill the missing data, in this paper, for the missing coordinates of the mounts' sample positions, according to the torque. In this paper, the missing position

coordinates of the sample mounts are derived from the torque roll axis (TRA) theory, which means that the elastic center of the mounts should fall on the torque axis. The angle between the inertia spindle and the torque axis should be slight, as shown in Figure 4.

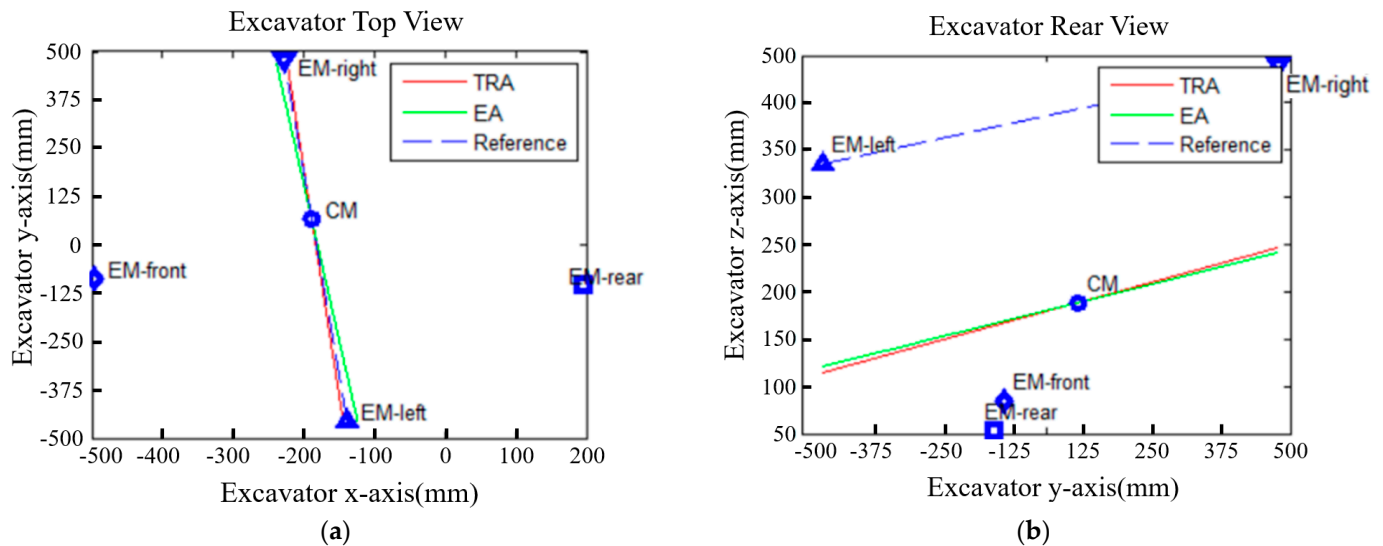


Figure 4. (a) Torque shaft top view position; (b) Torque shaft rear view position.

2. Data Correlation Analysis

Data correlation analysis refers to the integration of data distributed over multiple data stores. Data redundancy and tuple duplication need to be considered in data correlation analysis. Data redundancy can be detected using a correlation analysis, given some attributes, to measure the degree to which each attribute contains other attributes. The correlation matrix is a square matrix containing Pearson product-moment correlation coefficients, which measure the dependencies between pairs of powertrain parameters [31]. The correlation coefficient takes values in the range $[-1,1]$. A value of -1 indicates a perfect negative correlation between two features. Conversely, a value of 1 indicates a positive correlation. The Pearson correlation coefficient can be considered the product of the covariance between the calculated features and the target divided by the standard deviation.

$$r = \frac{\sum_{i=1}^n [(x^{(i)} - \mu_x)(y^{(i)} - \mu_y)]}{\sqrt{\sum_{i=1}^n (x^{(i)} - \mu_x)^2} \sqrt{\sum_{i=1}^n (y^{(i)} - \mu_y)^2}} = \frac{\sigma_{xy}}{\sigma_x \sigma_y} \quad (9)$$

The correlation matrix between the features of the cab mount system is calculated according to the Pearson correlation coefficient calculation theory, as shown in Figure 5. The redder the color that the matrix thermal indicates, the more significant the correlation. From the figure, it can be concluded that the mass m and the rotational inertia I_{xx} , I_{yy} , I_{zz} , I_{xy} are more correlated than other features, which matches with the engineering reality; in addition, the right front suspension mass center y direction coordinate C_{ay} and the left front suspension mass center y directional coordinates C_{ay} and left front mount y directional coordinates C_{by} contain each other to a greater extent, and the correlation coefficient reaches -0.945 . It is known that the original input parameter features have some redundancy, so it is necessary to reduce the dimensionality of the input data.

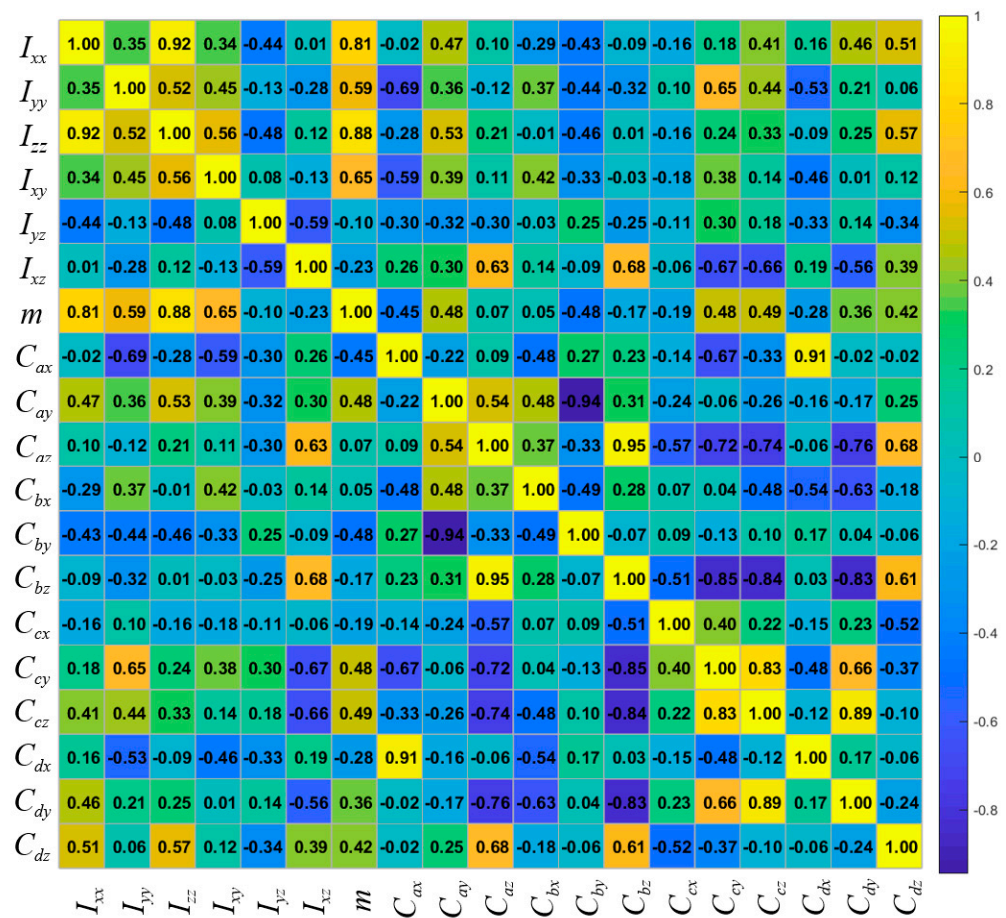


Figure 5. Correlation matrix between features.

3. Data Dimensionality Reduction

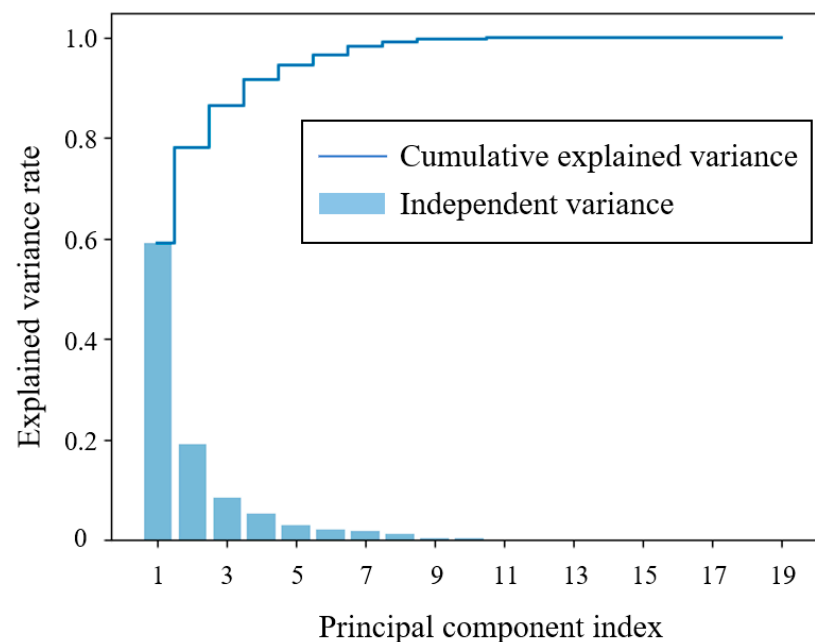
Data dimensionality reduction refers to ensuring the integrity of the original data and representing the data set in a more diminutive form. The performance of the mining model built on the normalized data set will be better. Let us suppose we can filter out some essential features from all the features so that the subsequent mining process only builds the model on some of the features. In that case, the model will not have a dimensional disaster, and thus the performance will be better. The main difference is that feature selection is intended to remove some “irrelevant features” or “redundant features” and select some “important features.” The standard feature selection algorithms can be divided into three types: filter, wrapper, and embedding, while feature extraction can be understood as data compression, which is the conversion or projection of data into a new feature space. The commonly used feature extraction techniques are principal components analysis (PCA), linear discriminant analysis (LDA) as a supervised dimensionality reduction technique to maximize differentiability, and kernel principal component analysis (KPCA) as a nonlinear dimensionality reduction technique.

PCA is a very effective unsupervised method for data compression, simplifying model complexity and avoiding model overfitting while maintaining the most relevant information [32]. PCA is an orthogonal linear transformation technique that aims to find the direction in which the maximum variance exists in high-dimensional data, and to transform the original sample data into a new space whose dimensionality is equal to or less than that of the original space. The process of principal component analysis is shown in Table 2.

Table 2. Principal component analysis process.

Input: sample set $D = \{x_1, x_2, \dots, x_m\}$; low dimensional space dimension d''
Process:
1. All samples are decentered: $x_i \leftarrow x_i - 1/m \left(\sum_{i=1}^m x_i \right)$
2. Calculate the covariance matrix XX^T of the samples
3. Eigenvalue decomposition of the covariance matrix XX^T
4. Take the largest d'' eigenvalues corresponding to the eigen components
Output: projection matrix $W^* = (w_1, w_2, \dots, w_d')$

As the feature dimension of the mount stiffness prediction model is high relative to the sample size, the model is prone to overfitting. The way to alleviate this “dimensional disaster” is to reduce the dimensionality of the data, optimize the storage space, improve computational efficiency, and improve the prediction performance. Therefore, PCA is applied to transform the problem into solving the eigenvalues and eigenvectors of the covariance matrix to find $n(n < 19)$ new variables, which are linear combinations of the original set of features and maximize the information of the powertrain, and these new variables become “principal components.” First, all the samples are standardized to construct a 19*19 dimensional covariance matrix. The eigenvectors and eigenvalues of the matrix are found as the principal components and the magnitude of the principal components, from which 19 eigenvectors and eigenvalues are obtained. The variance-explained ratio of the eigenvalues is the ratio of the eigenvalues to the total value. Then, the cumulative explained variance graph is established, as shown in Figure 6.

**Figure 6.** Cumulative explained variance plot.

The bars in Figure 6 represent the independent variable of each principal component, and the dashes represent the cumulative variance rate. The analysis shows that the cumulative explained variance rate of the 10 first principal components has reached 99.9%, i.e., these 10 “new variables” can capture 99.9% of the variance of the original data set, so the first 10 principal components are extracted as the new feature set, thus reducing the feature set to 10 dimensions and achieving the purpose of simplifying the model and preventing overfitting.

3.2. MRFs Prediction Results

The performance of MRFs models is usually evaluated by the goodness-of-fit (R^2) and root means square error (RMSE). The better the model performance, the closer the goodness-of-fit is to 1. On the contrary, the worse the model performance, the closer the goodness-of-fit is to 0. In some cases, the goodness-of-fit may be harmful, i.e., the model considers that the predictor variables do not have a regression relationship but are randomly distributed. The root mean square error can amplify the value of the more significant prediction deviation and compare the stability of different models. It can capture a part of the model's response variance function to reflect that the model performs better. Root mean square error and goodness-of-fit are commonly used regression model evaluation indicators, where the root mean square error and goodness-of-fit are expressed as:

$$RMSE = \sqrt{\frac{1}{N} \sum_{i=1}^N (y_i - \hat{y}_i)^2} \quad (10)$$

$$R^2 = 1 - \frac{\sum_{i=1}^N (\hat{y}_i - y_i)^2}{\sum_{i=1}^N (\bar{y}_i - y_i)^2} \quad (11)$$

In the above equation: N is the number of samples, y_i is the actual value, \bar{y}_i is the average value, and \hat{y}_i is the predicted value.

Model training was performed according to the MRFs algorithm, and 12 stiffnesses were predicted for the four-point mounts. As shown in Table 3, some samples were taken for the static stiffness of the cab mounts after optimization by MRFs. The predicted results of each model are compared with the real values, as shown in Figure 7. As shown in Table 4, before data cleaning, the RMSE, R^2 , and data dimension were 9.7681, 0.9924, and 19, respectively, and after data cleaning and dimensionality reduction, the RMSE, R^2 , and data dimension were 8.6524, 0.9946, and 10, respectively. The processed data not only improved the efficiency of model operation but also reduced the root mean square error and improved the goodness-of-fit.

Table 3. Cab mount static stiffness after optimization by MRFs.

Direction	Right Front Mount Stiffness (N/mm)	Left Front Mount Stiffness (N/mm)	Right Rear Mount Stiffness (N/mm)	Left Rear Mount Stiffness (N/mm)
x	702	706	697	694
y	690	700	701	707
z	960	890	999	865

Table 4. MRFs model predicts the RMES and R^2 results of the training set.

	RMES	R^2	Dimensionality
Raw data	9.7681	0.9924	19
Preprocessed data	8.6524	0.9946	10

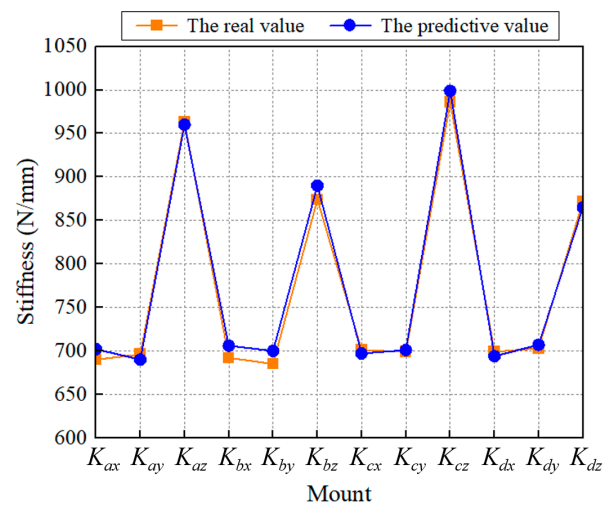


Figure 7. Test sample by MRFs model: the real value vs. the predicted value.

3.3. Calibration of Evaluation Objectives

The model is evaluated in terms of RMSE and R^2 , which assess the closeness of the predicted value to the actual value from a numerical point of view. A cab mount system with good vibration isolation performance requires a reasonable matching of the stiffnesses of the four mounts in three directions. In the actual optimization process of the mount system, the individual mounts' stiffnesses are matched with the cab vibration comfort improvement goal. Therefore, the decoupling rate and vibration isolation rate evaluation indices should be introduced as the boundary conditions of the multi-output regression model to further evaluate the constraints of the indices on the model from the engineering application level. The six-DOF model is established by using the view module in ADAMS [33], which replaces the construction machinery cab assembly with a rectangular mass model, represents the mounts with bushing units, and calculates the decoupling and vibration isolation rates [34,35].

1. Decoupling Rate Analysis

Usually, the decoupling degree of the system is expressed by the modal decoupling rate. At a particular order frequency, if its modal energy accounts for more than 98% of the total energy, this modal energy is powerful, implying that the mode is dominant at this frequency. If the decoupling rate of each order modal is 100%, it proves that each modal is independent of and does not affect the other. The systems on the excavators are interconnected with each other, so it is required that each order of the system modal must be separated. Otherwise, the vibration coupling will occur, which increases the difficulty of isolating the vibration. In the design and development process of the excavator cab mount system, it is necessary to reasonably match each order of modal frequency and make the vibration on each degree of freedom independent of each other. That is, the decoupling degree is high, and in the actual design process, the modal decoupling method is commonly used [36].

Modal decoupling is also called energy decoupling. From the energy point of view, the decoupling of the system along the coordinate direction consists in all the work being performed by the excitation force acting in that direction, which is converted into the energy of the system in that direction. In other words, the excitation force along a specific direction only causes the vibration in that direction. The modal decoupling rate is calculated as follows.

(1) The differential equations for the free vibration of the suspension system are established to obtain the intrinsic frequency and the principal vibration mode of the system.

(2) By calculating the kinetic energy assigned to a mode in generalized coordinates, the kinetic energy assigned in the k th generalized coordinate is expressed as:

$$T_k = \frac{\omega_i^2}{2} m_{kl} (A_i)_k (A_i)_t \quad (12)$$

In the above equation, ω_i is the i th-order intrinsic frequency; A_i is the i th-order principal vibration type of the system; $(A_i)_k$ and $(A_i)_t$ are the k th element and the l th element of the system, respectively; m_{kl} is the k th row and l th column element of the bit system mass matrix.

(3) The percentage of the total kinetic energy assigned to a mode in generalized coordinates is calculated as follows:

$$T_p = \frac{\sum_{k=1}^6 m_{kl} (A_i)_k (A_i)_t}{\sum_{l=1}^6 \sum_{k=1}^6 m_{kl} (A_i)_k (A_i)_t} \times 100\% \quad (13)$$

Table 5 shows the cab mount stiffnesses for the original construction machinery. The magnitude of the natural frequency and decoupling rate of the original cab mounts are also shown Table 6. Among them, the maximum decoupling rate in the Z direction is 99.85%, and the minimum decoupling rate in the R_x direction is 48.88%.

Table 5. Original cab mounts' static stiffness.

Direction	Right Front Mount Stiffness (N/mm)	Left Front Mount Stiffness (N/mm)	Right Rear Mount Stiffness (N/mm)	Left Rear Mount Stiffness (N/mm)
x	699	700	706	693
y	699	700	706	693
z	221	226	219	226

Table 6. Original cab mount system natural frequency and decoupling rate.

Modal Order Number	Natural Frequency (Hz)	Decoupling Rate (%)						
		X	Y	Z	R_x	R_y	R_z	Max
1	1.89	0.00	50.22	0.07	49.71	0.00	0.00	50.22
2	3.61	47.12	0.00	0.08	0.00	52.80	0.01	52.80
3	5.89	0.05	0.05	99.85	0.02	0.03	0.00	99.85
4	12.36	0.58	1.67	0.00	1.10	0.71	95.94	95.94
5	13.94	52.06	0.33	0.00	0.29	46.30	1.03	52.06
6	14.73	0.19	47.73	0.00	48.88	0.17	3.03	48.88

Table 7 shows the magnitude of the natural frequencies and decoupling rates of the cab mount system after optimization by MRFs. The analysis of the optimized natural frequencies shows that the MRFs model satisfies the frequency interval of each order greater than 1 Hz, where the maximum decoupling rate is 99.87% in the Z direction, and the minimum decoupling rate is 57.47% in the R_x direction.

Table 7. Natural frequency and decoupling rate of cab mounts after optimization by MRFs.

Modal Order Number	Natural Frequency (Hz)	Decoupling Rate (%)						
		X	Y	Z	R_x	R_y	R_z	Max
1	5.42	0.01	58.40	0.01	41.57	0.00	0.01	58.40
2	7.52	75.03	0.00	0.02	0.00	24.86	0.08	75.03
3	12.40	0.01	0.91	0.00	0.71	0.15	98.21	98.21
4	14.34	0.18	0.29	99.08	0.24	0.21	0.01	99.87
5	15.35	0.00	40.39	0.53	57.47	0.01	1.60	57.47
6	16.40	24.78	0.00	0.36	0.00	74.77	0.09	74.77

2. Vibration Isolation rate Analysis

The z-directional excitation of the cab mount system is shown in Figure 8. The vibration isolation rate is widely defined as the acceleration of the main and passive ends of the mounts to calculate, and the engineering vibration isolation rate can be expressed as:

$$T = 20 \log \left(\frac{A_{active}}{A_{passive}} \right) \quad (14)$$

where T is the vibration isolation rate, A_{active} is the vibration acceleration of the active end, and $A_{passive}$ is the vibration acceleration of the passive end.

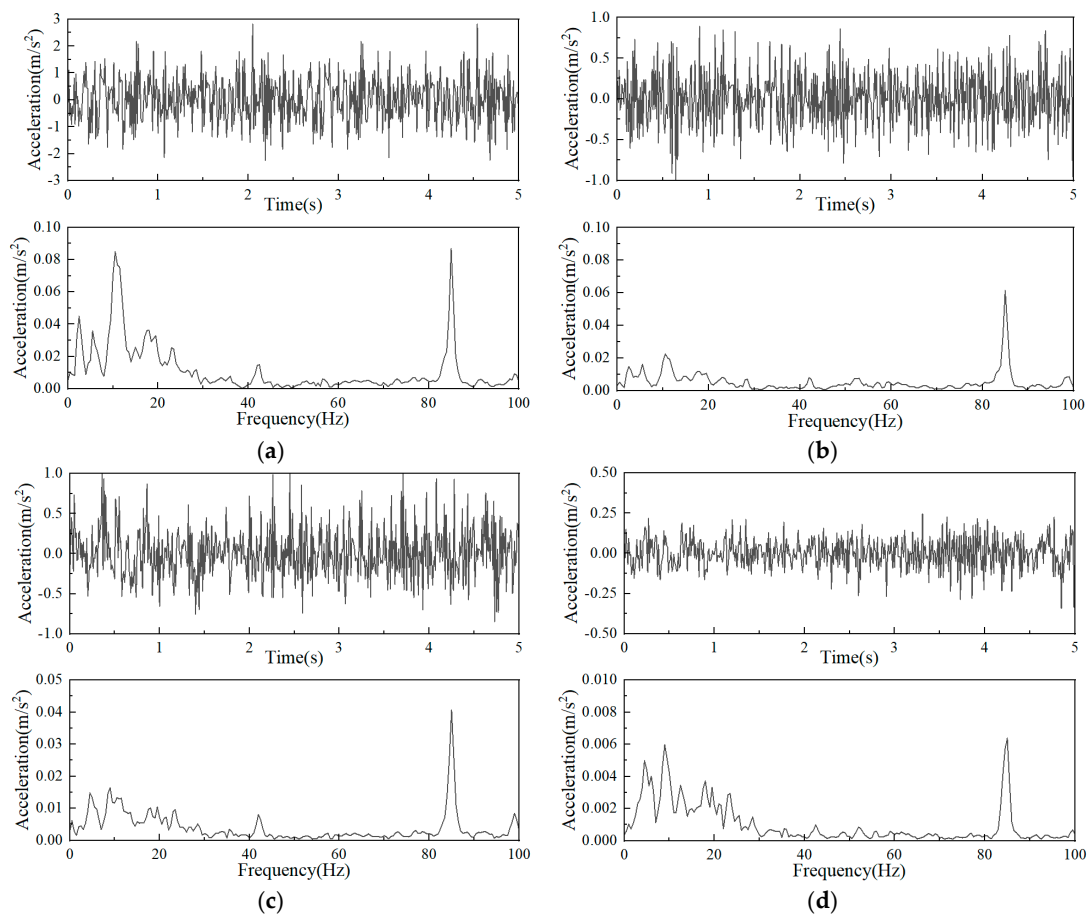


Figure 8. Time and frequency domain excitation of: (a) the right front mount system in the z-direction; (b) the left front mount system in the z-direction; (c) the right rear mount system in the z-direction; (d) the left rear mount system in the z-direction.

The vibration isolation rates of the original cab mounts are shown in Figure 9, where the vibration isolation rates in the right front, left front, right rear, and left rear Z directions are 3.57 dB, 9.90 dB, 0.36 dB, and 5.48 dB, respectively, and the vibration isolation rates of the cab mounts optimized by MRFs are shown in Figure 10, where the vibration isolation rates in the right front, left front, right rear, and left rear Z directions are 5.67 dB, 12.00 dB, 2.45 dB, and 7.58 dB, respectively. Compared with the original cab mount stiffnesses, the vibration isolation rate is more visibly improved.

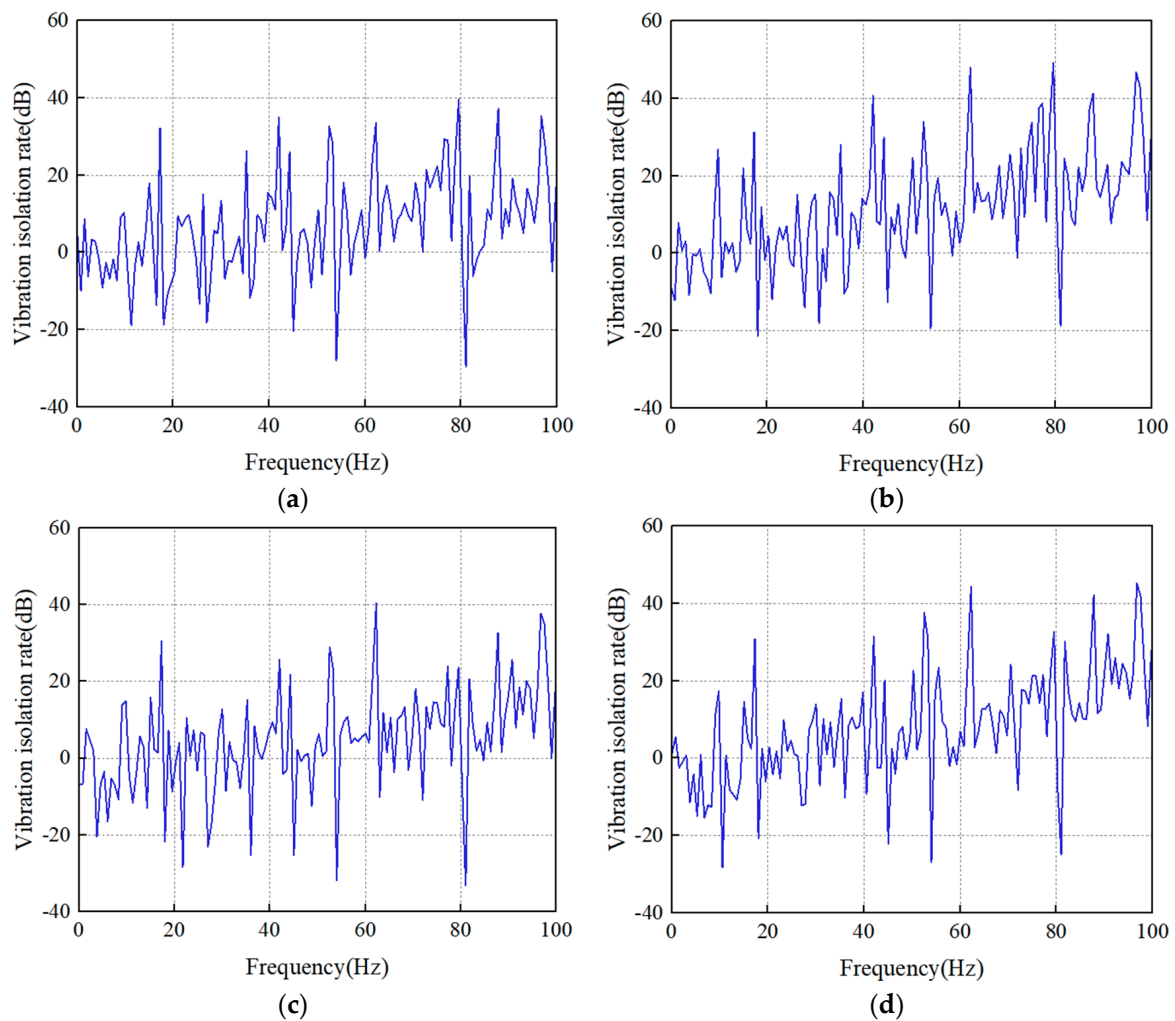


Figure 9. Original cab mounts: (a) z-directional vibration isolation rate of the right front mounts; (b) z-directional vibration isolation rate of the left front mounts; (c) z-directional vibration isolation rate of the right rear mounts; (d) z-directional vibration isolation rate of the left rear mounts.

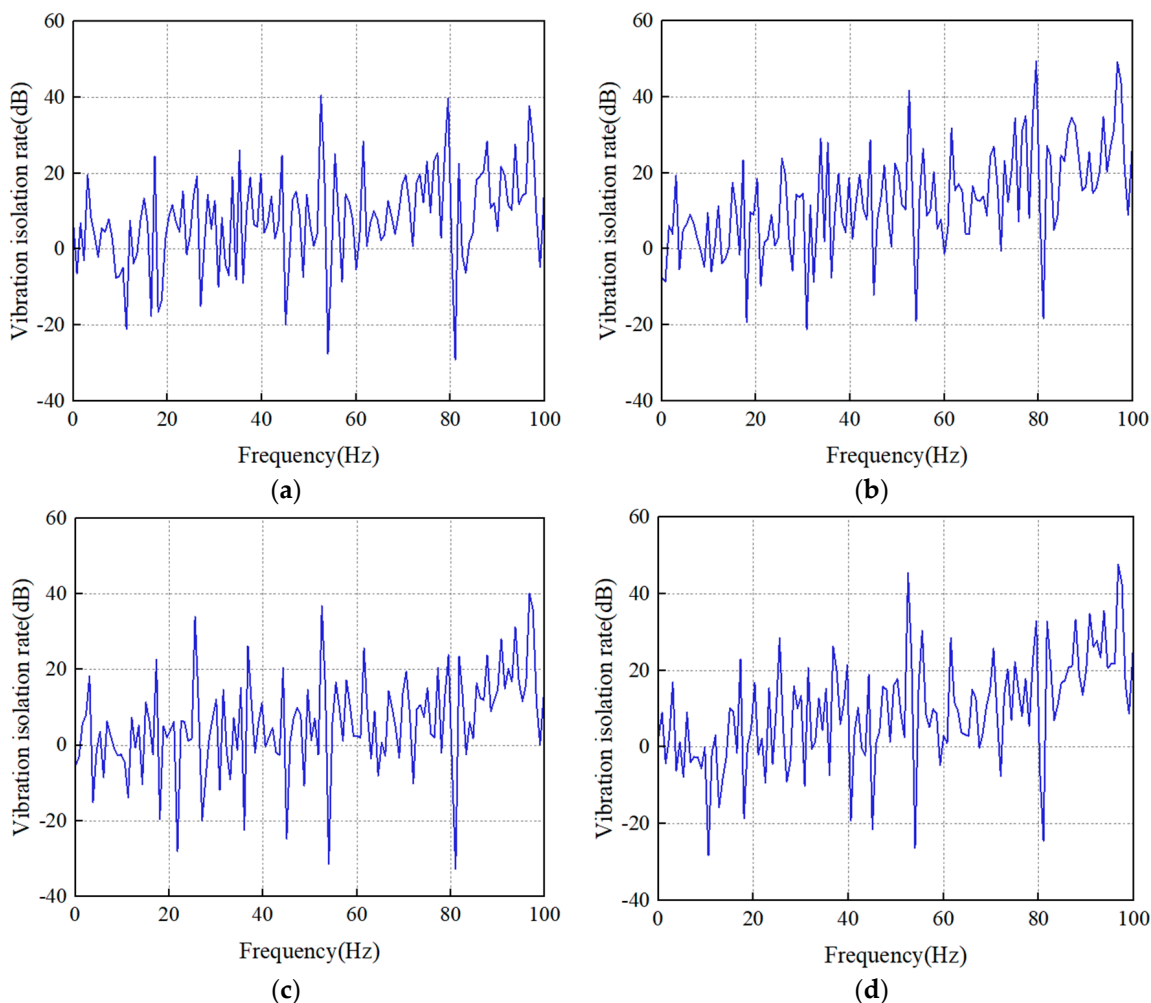


Figure 10. Cab mounts optimized by MRFs: (a) z-directional vibration isolation rate of right front mounts; (b) z-directional vibration isolation rate of left front mounts; (c) z-directional vibration isolation rate of right rear mounts; (d) z-directional vibration isolation rate of left rear mounts.

3.4. Comparison of Method Effects

MRFs are multi-output regression algorithms, including multi-layer perception regression (MLPR) and multi-output support vector machine regression (multi-SVR), etc.

Multi-layer perception regression (MLPR) consists of three parts: the input layer, the hidden layer, and the output layer. All nodes in the hidden and output layers are neurons using a nonlinear activation function. In addition, the hidden layer can be composed of multiple layers of neurons. The units of each layer are fully connected, and the output of the previous layer is transformed into the input value of the next layer by the activation function. The operation continues backward until it is counted to the output layer, where the output value of the hidden layer unit is:

$$y_{pj} = f_j \sum_i w_{ij} x_{pj} - \theta_j \tag{15}$$

In the above equation, w_{ij} is the connection weight of the i th node of the input layer and the j th node of the hidden layer; x_{pj} is the value of the i th input unit of the p th sample; θ_j is the threshold of the j th node; and f_j is the activation function, which can usually be the Tanh function, Sigmoid function, and Relu function; the expressions of which are, respectively:

$$\text{sigmoid}(x) = \frac{1}{1 + e^{-x}} \tag{16}$$

$$\text{Tanh}(x) = \frac{e^x - e^{-x}}{e^x + e^{-x}} \tag{17}$$

$$\text{Relu}(x) = \begin{cases} x, & x > 0 \\ 0, & x \leq 0 \end{cases} \tag{18}$$

In this thesis, the MLPR network consists of three layers (an input layer, a hidden layer, and an output layer) in nonlinear activation mode. The input layer has 19 nodes corresponding to the 19 input parameters of the cab, the hidden layer is set up with 17 neurons, and the output layer has 12 neurons corresponding to the stiffness values in a total of 12 directions for the four mounts. When the network parameters are learned based on the training data, all the weights and deviations of the associations between the cab input parameters and the stiffness are updated. When new data are applied, the predicted values are calculated based on the learned weights and deviations. Table 8 shows the construction machinery cab mount stiffness after optimization by MLPR. Table 9 shows the magnitude of the natural frequency and decoupling rate of the construction machinery cab system after optimization by MLPR. The vibration isolation rate of the cab mount system after optimization by MLPR is shown in Figure 11. Among them, the maximum decoupling rate in the Z direction is 99.87%, and the minimum decoupling rate in the R_x direction is 52.03%. The vibration isolation rates in the Z direction for the right front, left front, right rear, and left rear are 2.07 dB, 8.40 dB, 1.14 dB, and 3.98 dB, respectively.

Table 8. Static stiffness of cab mounts after optimization by MLPR and Multi-SVR.

Method	Direction	Right Front Mounts Stiffness (N/mm)	Left Front Mounts Stiffness (N/mm)	Right Rear Mounts Stiffness (N/mm)	Left Rear Mounts Stiffness (N/mm)
MLPR	x	702	699	695	690
	y	697	693	703	696
	z	431	403	397	450
Multi-SVR	x	702	695	700	699
	y	693	694	698	690
	z	637	605	589	629

Table 9. Natural frequency and decoupling rate of cab mounts after optimization by MLPR and multi-SVR.

Method	Modal Order Number /	Natural Frequency (Hz)	Decoupling Rate (%)						
			X	Y	Z	R_x	R_y	R_z	Max
MLPR	1	3.06	0.05	53.02	0.06	46.83	0.05	0.00	53.02
	2	5.63	57.96	0.05	0.03	0.04	41.89	0.02	57.96
	3	9.65	0.04	0.09	99.87	0.00	0.00	0.00	99.87
	4	12.36	0.12	1.33	0.00	0.92	0.39	97.23	97.23
	5	14.63	41.73	0.14	0.01	0.18	57.56	0.39	57.56
	6	14.91	0.11	45.37	0.03	52.03	0.10	2.36	52.03
Multi-SVR	1	3.66	0.02	55.16	0.07	44.73	0.01	0.00	55.16
	2	6.54	65.25	0.02	0.08	0.01	34.61	0.04	65.25
	3	11.67	0.18	0.24	99.54	0.02	0.02	0.00	99.54
	4	12.34	0.02	1.26	0.01	0.96	0.27	97.48	97.48
	5	15.04	0.03	43.28	0.19	54.23	0.11	2.17	54.23
	6	15.26	34.50	0.05	0.12	0.04	64.98	0.31	64.98

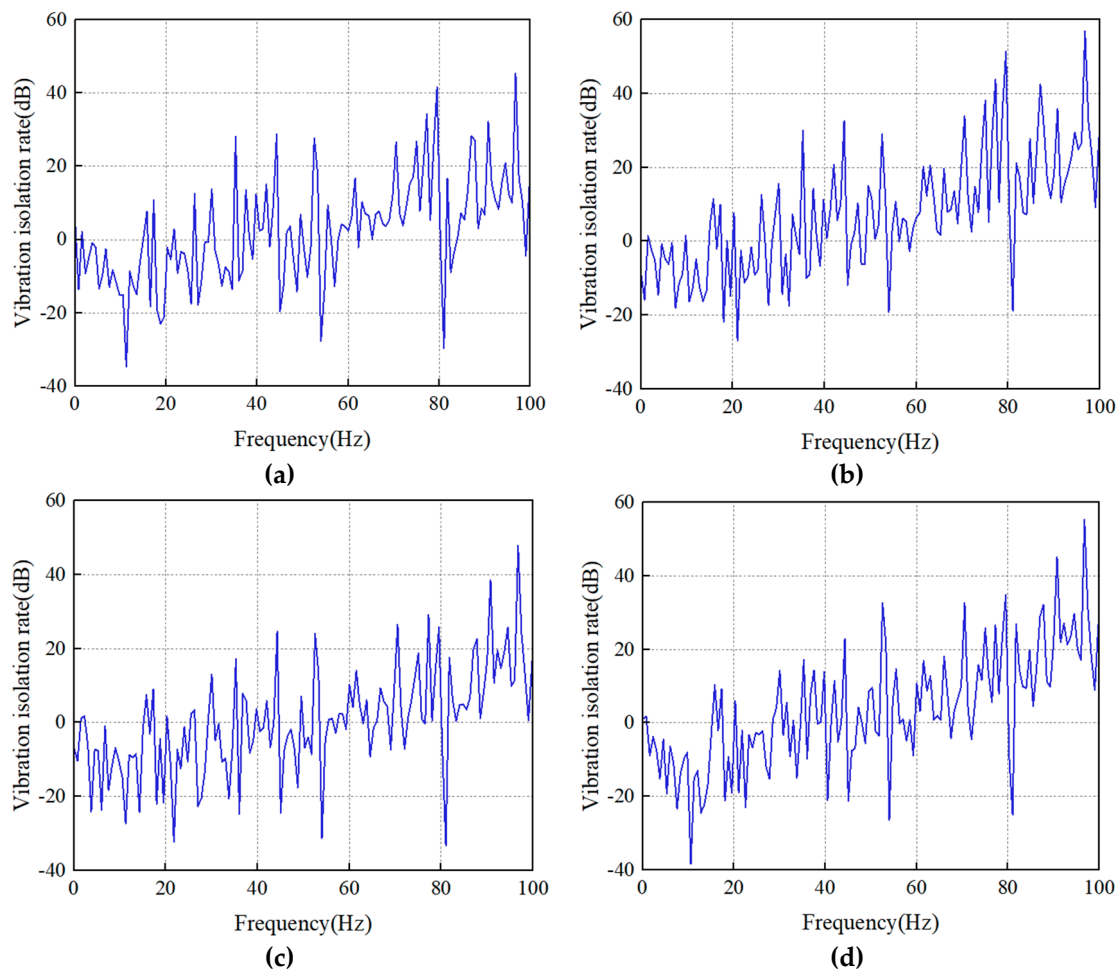


Figure 11. Optimized rear cab mounts by MLPR: (a) z-directional vibration isolation rate of right front mounts; (b) z-directional vibration isolation rate of left front mounts; (c) z-directional vibration isolation rate of right rear mounts; (d) z-directional vibration isolation rate of left rear mounts.

The support vector machine regression algorithm is only applicable to single-output systems. When dealing with suspension stiffness prediction, constructing a series of single-output support vector machine models is used to build a multi-SVR for mount stiffness. Support vector machine regression (SVR) is a typical least-squares regression model, which extends the support vector machine algorithm to the regression problem. The loss value of the traditional regression algorithm is the difference between the model output value and the real value. In contrast, the support vector machine regression algorithm allows for the model output value to have a specific difference value, i.e., the loss calculation only starts when the difference between the model output value and the real value is less than ε . Thus, the support vector machine regression problem can be formalized as:

$$\min_{w,b} \frac{1}{2} \|w\|^2 + C \sum_{i=1}^m l_{\varepsilon}(f(x_i) - y_i) \quad (19)$$

In the above equation, w is the normal vector; b is the displacement vector; C is the regularization parameter; ε denotes the deviation; and $l_{\varepsilon}(z)$ is the insensitive loss function of the following form:

$$l_{\varepsilon}(z) = \begin{cases} 0, & \text{if } |z| \leq \varepsilon \\ |z| - \varepsilon, & \text{otherwise} \end{cases} \quad (20)$$

For the support vector machine model, the kernel range must be set as linear kernel, polynomial kernel, Gaussian kernel, and Sigmoid kernel, the gamma parameter range must

be set as $(10^{-4}, 10^3)$, and the penalty factor responds to the penalty degree of the algorithm on the sample data, for example, if C is too small, the training error is significant, and if the penalty factor C is too large, the generalization ability of the model becomes poor, so the C parameter range must be set as $(10^{-4}, 10^3)$. The grid search method is used to determine the best combination of parameters for the model, i.e., the kernel function is Gaussian kernel, the gamma value is 0.05, and the penalty factor is 0.1. In Table 8 is shown the construction machinery cab mount stiffness optimized by regression through multi-SVR. Table 9 shows the magnitude of the cab mount system's natural frequency and decoupling rate after optimization by multi-SVR. Figure 12 shows the vibration isolation rate of the cab mounts after optimization by multi-SVR. Among them, the maximum decoupling rate is 99.54% in the Z direction, and the minimum decoupling rate is 54.23% in the R_x direction. The right front, left front, right rear, and left rear Z direction vibration isolation rates are 1.95 dB, 8.28 dB, 1.26 dB, and 3.87 dB, respectively.

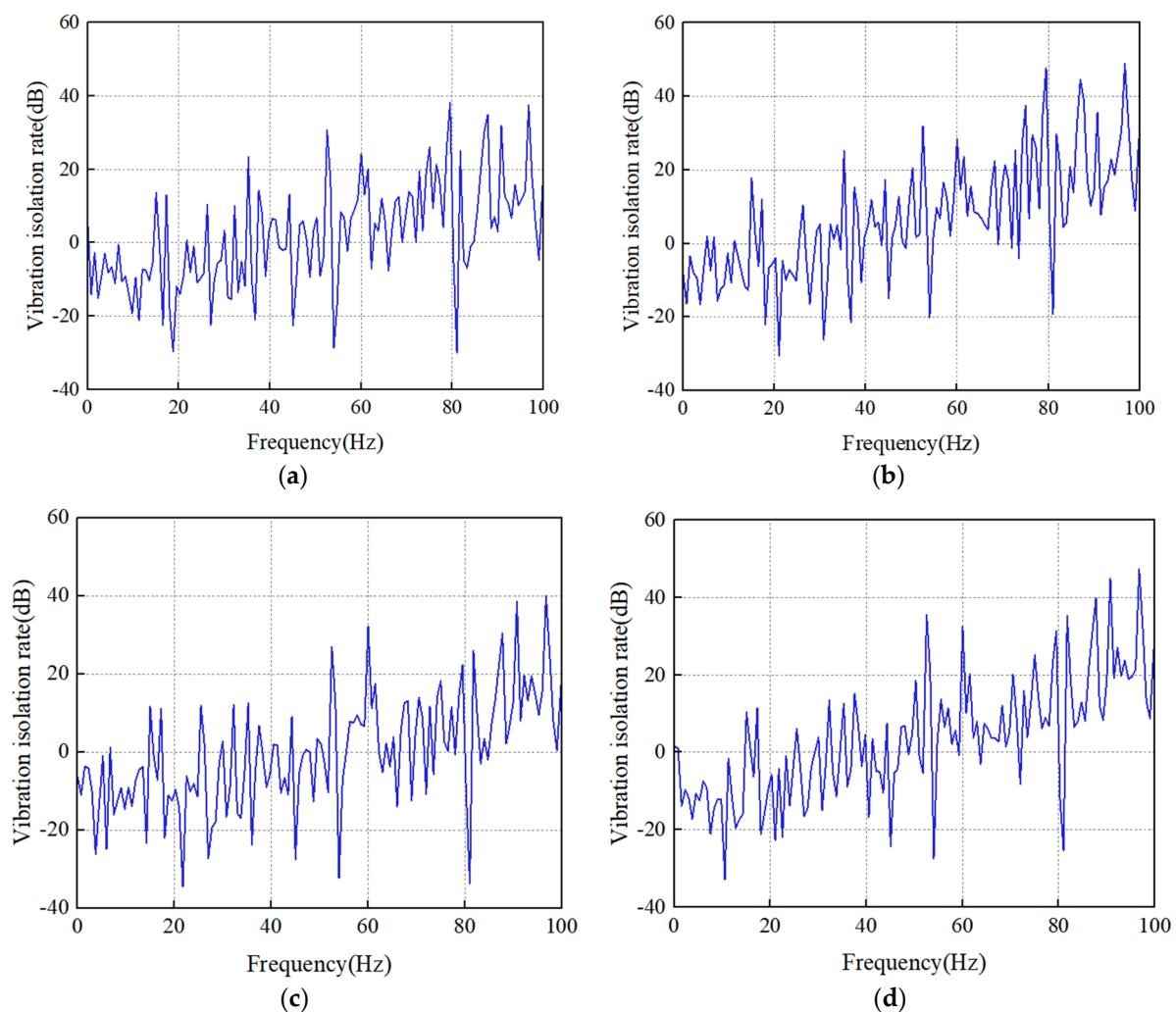


Figure 12. Optimization of rear cab mount system by multi-SVR: (a) z-directional vibration isolation rate of right front mount; (b) z-directional vibration isolation rate of left front mount; (c) z-directional vibration isolation rate of right rear mount; (d) z-directional vibration isolation rate of left rear mount.

The analysis of the natural frequencies of different prediction models shows that the MLPR and multi-SVR models do not meet the requirement of a modal frequency interval greater than 1 Hz at each order, and only the MRFs model meets the requirement. The optimized decoupling rate of the MRFs model is significantly higher than the original decoupling rate, and the decoupling rate is higher than the MLPR and multi-SVR models

in each direction of freedom. Analyzing the isolation rates of different prediction models, it is found that the optimized mount stiffness of the MLPR and multi-SVR models slightly decreases from the original state by 0–100 Hz due to the increased static stiffness. However, the optimized mount stiffness of the MRFs model increases more significantly from the original state by 0–100 Hz.

4. Conclusions

In this paper, data mining technology is introduced into the design of cab mounts of construction machinery. Avoiding the cost of mount stiffness prediction caused by significant data dimensions, the data preprocessing method sample data is optimized based on data cleaning, data correlation analysis, and data dimensionality reduction. Subsequently, the MRFs are used to predict the stiffness of the mount in multiple directions. At the same time, the system decoupling rate and vibration isolation rate engineering indices are introduced as boundary conditions for evaluation and optimization. The results show that the optimized stiffness of the cab with MRFs meets the natural frequency of each order greater than 1 Hz, and the optimized decoupling rate in the Z direction and R_x direction is improved compared with the original stiffness; compared to the original stiffness, the optimized vibration isolation rate of the MRFs is significantly improved. In addition, MRFs are compared with the prediction results of MLPR and multi-SVR, and it is found that the MLPR and multi-SVR models do not satisfy the modal frequency interval of each order greater than 1 Hz, and only the MRFs model satisfies the requirements. The decoupling rate in each degree of freedom direction after optimization of the MRFs model is higher than that of the multi-SVR and MLPR models; moreover, only the MRFs model improves the vibration isolation rate significantly compared to the original state after optimization, while the other models even decrease in some directions. In summary, the advantages of MRFs for mount system stiffness prediction are highlighted. The drawbacks of traditional finite element design methods and traditional data mining methods, such as high development difficulty and low robustness, are solved to provide guidance directions for mount system stiffness prediction.

Author Contributions: C.Z.; writing—review and editing; H.W.; writing—original draft preparation; X.N.; visualization; D.Z.; validation; Y.B.; methodology; H.H.; conceptualization, funding acquisition. All authors have read and agreed to the published version of the manuscript.

Funding: This research was funded by the National Natural Science Foundation of China (No. 51905408), the SWJTU Science and Technology Innovation Project, grant number 2682022CX008, 2682021ZTPY068.

Data Availability Statement: Not applicable.

Conflicts of Interest: The authors declare no conflict of interest.

References

1. EN 474-7:2007+A1:2009; Earth-Moving Machinery—Safety—Part 7: Requirements for Scrapers. BSI: London, UK, 2009.
2. Cho, S. Configuration and sizing design optimisation of powertrain mounting systems. *Int. J. Veh. Des.* **2000**, *24*, 34–47. [[CrossRef](#)]
3. Nova, M.; Berria, C.; Tamburro, A.; Pisino, E. *Noise and Vibration Reduction for Small/Medium Car-Market Segment: An Innovative Approach for Engineering Design and Manufacturing*; IMechE: Birmingham, UK, 1997.
4. Huang, H.; Huang, X.; Ding, W.; Yang, M.; Yu, X.; Pang, J. Vehicle interior vibro-acoustical comfort optimization using a multi-objective interval analysis method. *Expert Syst. Appl.* **2022**, *213*, 119001. [[CrossRef](#)]
5. Ahmadian, M.; Patricio, P.S. Effect of Panhard Rod Cab Suspensions on Heavy Truck Ride Measurements. *SAE Trans.* **2004**, *113*, 551–559. [[CrossRef](#)]
6. De Temmerman, J.; Deprez, K.; Anthonis, J.; Ramon, H. Conceptual Cab Suspension System for a Self-propelled Agricultural Machine, Part 1: Development of a Linear Mathematical Model. *Biosyst. Eng.* **2004**, *89*, 409–416. [[CrossRef](#)]
7. Huang, H.; Huang, X.; Ding, W.; Yang, M.; Fan, D.; Pang, J. Uncertainty optimization of pure electric vehicle interior tire/road noise comfort based on data-driven. *Mech. Syst. Signal Process.* **2022**, *165*, 108300. [[CrossRef](#)]
8. Hong, L.; Li, Y.; He, M.; Zhao, C.; Li, M. An algorithm to calibrate ionic isotopes using data mining strategy in hyphenated chromatographic datasets from herbal samples. *J. Chromatogr. A* **2019**, *1613*, 460668. [[CrossRef](#)] [[PubMed](#)]

9. Gordan, M.; Razak, H.A.; Ismail, Z.; Ghaedi, K.; Tan, Z.X.; Ghayeb, H.H. A hybrid ANN-based imperial competitive algorithm methodology for structural damage identification of slab-on-girder bridge using data mining. *Appl. Soft Comput.* **2020**, *88*, 106013. [[CrossRef](#)]
10. Li, X.F.; Yang, X.X. A review of elastic constitutive model for rubber materials. *China Elastomerics* **2005**, *15*, 50–58.
11. Müller, M.; Eckel, H.-G.; Leibach, M.; Bors, W. Reduction of Noise and Vibration in Vehicles by an Appropriate Engine Mount System and Active Absorbers. *SAE Trans.* **1996**, *105*, 146–157. [[CrossRef](#)]
12. Le Fol, M.; Robic, P. Hydroelastic Support in Particular for the Suspension of a Power Unit in the Body of a Motor Vehicle. US4893797A. U.S. Patent 4,856,750, 15 August 1989.
13. Foumani, M.S.; Khajepour, A.; Durali, M. *Application of Shape Memory Alloys to a New Adaptive Hydraulic Mount*; SAE International: Warrendale, PA, USA, 2002. [[CrossRef](#)]
14. Roy, J.; Law, E.H. Effect of Cab Suspension Configuration and Location on Tractor Semi-Trailer Driver Comfort. *SAE Int. J. Commer. Veh.* **2016**, *9*, 405–416. [[CrossRef](#)]
15. Neto, A.J.; Fernandes, C.G.; Pedroso, R.D.; Vianna, E.P. *Trucks Ride Simulation—Tuning Optimization*; SAE International: Warrendale, PA, USA, 2010. [[CrossRef](#)]
16. Soliman, A.M.A. *Improvement of the Truck Ride Comfort via Cab Suspension*; SAE International: Warrendale, PA, USA, 2008. [[CrossRef](#)]
17. Deng, Z. Model Identification of Magneto-Rheological Mount Based on Genetic Algorithms and BP Neural Network. *J. Univ. Electron. Sci. Technol. China* **2014**, *43*, 955–960.
18. Fang, Y.; Zhang, T.; Chen, F.; Guo, R. Sound quality prediction of electric power train noise based on particle swarm optimization and support vector machine. *J. Xian Jiaotong Univ.* **2016**, *50*, 41–46.
19. Cao, M.; Wang, K.W.; Fujii, Y.; Tobler, W.E. Advanced hybrid neural network automotive friction component model for powertrain system dynamic analysis. Part 2: System simulation. *Proc. Inst. Mech. Eng. Part D J. Automob. Eng.* **2004**, *218*, 845–857. [[CrossRef](#)]
20. Cichosz, P.; Pawelczak, L. Imitation learning of car driving skills with decision trees and random forests. *Int. J. Appl. Math. Comput. Sci.* **2014**, *24*, 579–597. [[CrossRef](#)]
21. Cerrada, M.; Zurita, G.; Cabrera, D.; Sánchez, R.; Artés, M.; Li, C. Fault diagnosis in spur gears based on genetic algorithm and random forest. *Mech. Syst. Signal Process.* **2016**, *70*, 87–103. [[CrossRef](#)]
22. Lu, Y.; Li, Y.; Xie, D.; Wei, E.; Bao, X.; Chen, H.; Zhong, X. The Application of Improved Random Forest Algorithm on the Prediction of Electric Vehicle Charging Load. *Energies* **2018**, *11*, 3207. [[CrossRef](#)]
23. Xie, J.X.; Le Wang, X.; Liu, C. Simulation and Optimization Design Based on Adams Engine Mounting System. *Appl. Mech. Mater.* **2014**, *686*, 567–572. [[CrossRef](#)]
24. Pobedin, A.V.; Dolotov, A.A.; Shekhovtsov, V.V. Decrease of the vibration load level on the tractor operator working place by means of using of vibrations dynamic dampers in the cabin suspension. *Procedia Eng.* **2016**, *150*, 1252–1257. [[CrossRef](#)]
25. Xu, X.; Su, C.; Dong, P.; Liu, Y.; Wang, S. Optimization design of powertrain mounting system considering vibration analysis of multi-excitation. *Adv. Mech. Eng.* **2018**, *10*, 1687814018788246. [[CrossRef](#)]
26. Qigang, X.; Xiangdong, L.; Hong, G.; Haikui, L.; Yutang, L. Stand biomass model of Larix olgensis plantations based on multi-layer perceptron networks. *J. Beijing For. Univ.* **2019**, *41*, 97–107. [[CrossRef](#)]
27. Spyromitros-Xioufis, E.; Tsoumakas, G.; Groves, W.; Vlahavas, I. Multi-target regression via input space expansion: Treating targets as inputs. *Mach. Learn.* **2016**, *104*, 55–98. [[CrossRef](#)]
28. Soliman, A.M.A.; Gazaly, N.M.; Kadry, F.S. *Parameters Affecting Truck Ride Comfort*; SAE International: Warrendale, PA, USA, 2014. [[CrossRef](#)]
29. Wang, G.; Li, K.; Yang, J.; Liang, C. Simulation and vibration isolation optimization on the cab mount of a commercial vehicle. *Automot. Eng.* **2017**, *39*, 1081–1086.
30. Huang, H.; Wu, J.; Lim, T.C.; Yang, M.; Ding, W. Pure electric vehicle nonstationary interior sound quality prediction based on deep CNNs with an adaptable learning rate tree. *Mech. Syst. Signal Process.* **2021**, *148*, 107170. [[CrossRef](#)]
31. Lee, W.-M. *Python® Machine Learning*; John Wiley & Sons, Inc.: Hoboken, NJ, USA, 2019.
32. Loh, W.-Y. Classification and regression trees. *Wiley Interdiscip. Rev. Data Min. Knowl. Discov.* **2011**, *1*, 14–23. [[CrossRef](#)]
33. Wang, T.; Wang, L.; Wang, C.; Liu, T.; Yuan, L.; Zhang, T. Development in the Acquisition of Vehicle Loads Integrated with a Rigid and Flexible Multi-Body Model. *SAE Int. J. Commer. Veh.* **2014**, *7*, 163–169. [[CrossRef](#)]
34. Huang, H.B.; Li, R.X.; Yang, M.L.; Lim, T.C.; Ding, W.P. Evaluation of vehicle interior sound quality using a continuous restricted Boltzmann machine-based DBN. *Mech. Syst. Signal Process.* **2017**, *84*, 245–267. [[CrossRef](#)]
35. Hazra, S.; Reddy, K.J. A comparative study of properties of natural rubber and polyurethane-based powertrain mount on electric vehicle NVH performance. *Int. J. Veh. Noise Vib.* **2022**, *18*, 22–40. [[CrossRef](#)]
36. Huang, H.; Huang, X.; Ding, W.; Zhang, S.; Pang, J. Optimization of electric vehicle sound package based on LSTM with an adaptive learning rate forest and multiple-level multiple-object method. *Mech. Syst. Signal Process.* **2022**, *187*, 109932. [[CrossRef](#)]